

Diffusion in Ni-Based Single Crystal Superalloys with Density Functional Theory and Kinetic Monte Carlo Method

Min Sun¹, Zi Li², Guo-Zhen Zhu³, Wen-Qing Liu⁴,
Shao-Hua Liu⁵ and Chong-Yu Wang^{6,1,*}

¹ Central Iron & Steel Research Institute, Beijing 100081, China.

² Institute of Applied Physics and Computational Mathematics, Beijing 100088, China.

³ State Key Laboratory of Metal Matrix Composites, School of Materials Science and Engineering, Shanghai Jiao Tong University, Shanghai 200240, China.

⁴ Key Laboratory for Microstructures, Shanghai University, Shanghai 200444, China.

⁵ School of Materials Science and Engineering, Tsinghua University, Beijing 100084, China.

⁶ Department of Physics, Tsinghua University, Beijing 100084, China.

Communicated by Weinan E

Received 11 November 2015; Accepted (in revised version) 27 November 2015

Abstract. In the paper, we focus on atom diffusion behavior in Ni-based superalloys, which have important applications in the aero-industry. Specifically, the expressions of the key physical parameter – transition rate (jump rate) in the diffusion can be given from the diffusion theory in solids and the kinetic Monte Carlo (KMC) method, respectively. The transition rate controls the diffusion process and is directly related to the energy of vacancy formation and the energy of migration of atom from density functional theory (DFT). Moreover, from the KMC calculations, the diffusion coefficients for Ni and Al atoms in the γ phase (Ni matrix) and the γ' phase (intermetallic compound Ni_3Al) of the superalloy have been obtained. We propose a strategy of time stepping to deal with the multi-time scale issues. In addition, the influence of temperature and Al concentration on diffusion in dilute alloys is also reported.

PACS: 71.15.Mb, 61.43.Bn, 66.30.-h, 71.55.Ak

Key words: Diffusion behavior, transition rate, density functional theory, kinetic Monte Carlo method, superalloy.

1 Introduction

Diffusion in solids, a fundamental phenomenon in material science, involves the correlation behavior of atomic motion and multi-length and time scales. In this paper, we focus

*Corresponding author. Email addresses: cywang@mail.tsinghua.edu.cn (C.-Y. Wang), ilphysics@163.com (M. Sun)

on the factors influencing the properties of Ni-based superalloys doped with heavy element Re, which have important applications in the aero-industry [1–11]. Motivated by scientific interest in superalloys, our work concerns the density functional theory as well as the diffusion behavior in solids [12–18].

Diffusion in superalloys is closely related to the evolution of the structural system, which involves its phase stability and homogenization, as well as the precipitation and dissociation of phases. In particular, the diffusion of atoms directly influences the high temperature creep behavior and thermal oxidation properties; we need to understand its mechanism and to control the process. In metals and alloys, the diffusion mechanism concerns mainly point defects induced by thermal fluctuations. Vacancy mechanism has been considered as the dominant mechanism in metals [19]. In this work, we confine our study to the atomic jump process of diffusion in matrix Ni and its dilute substitutional binary alloy [19], and study the diffusion process in $L1_2$ intermetallic Ni_3Al via the sublattice vacancy mechanism [19–21] for Ni atoms and Al atoms.

Kinetic Monte Carlo (KMC) methods [22,23] are used in computations in many areas that study the dynamic behavior of systems with interacting particles. By describing the configuration transition process instead of calculating atom trajectories, the KMC method can provide a multi-time and multi-length scale description for the diffusion behavior of materials. For each step in the algorithm, an atomic transition process is chosen at random from a list of possible processes; the probability for each process is weighted by its transition rate (jump rate). A previous theoretical study [24] has shown that, under some general conditions, the KMC method simulates both the static and dynamic properties of model systems consistently and correctly. In contrast, molecular dynamics simulations describing the trajectories of individual atoms or molecules on potential energy are not computationally capable of probing large systems of interacting particles over long times. Thus, in a dynamics capacity, the KMC methods are an efficient means for studying diffusion that bridges density functional theory (DFT) and dynamic approaches. The predictive power of the KMC methods has been demonstrated for a wide range of experimental phenomena, such as vacancy diffusion [25], phase transition [26], domain growth [27], and adatom diffusion on surface [28–30]. In addition, these methods are of crucial importance to the study of electron transport in organic materials [31,32].

In this paper, the theoretical basis is on the harmonic transition state theory (HTST) [22,23,32,33] and to calculate KMC transition rate with DFT. The HTST transition rate trends to a very exact rate in most solid materials for solid state diffusive processes [34,35].

2 Construction of calculation model with relevant experiments

Motivated by scientific interest and the importance of properties of Re-doped Ni-based superalloys (considering the solubility of Re from the phase diagram of Ni-Al-Re system and the lower content of Re, the more interesting for superalloys), as indicated by exper-

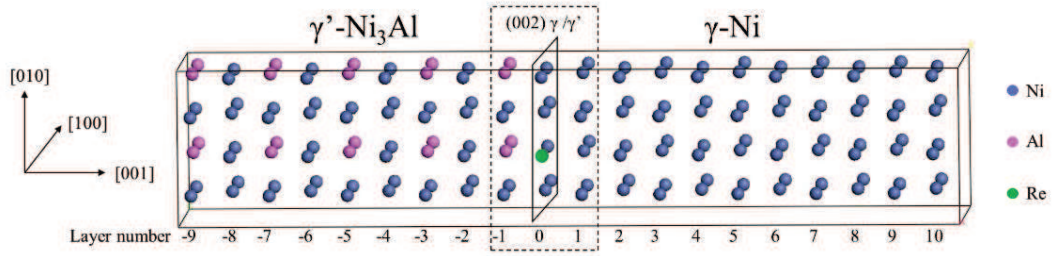


Figure 1: Diagram of the 160-atom supercell model ($2a_0 \times 2a_0 \times 10a_0$) viewed along the $\langle 001 \rangle$ direction. Periodic boundary conditions are applied along the $[100]$ and $[010]$ directions whereas a 12 \AA vacuum layer is imposed in the $[001]$ direction. The supercell is divided equally by a $(002) \gamma\text{-}\gamma'$ connecting layer (number 0), with the $\gamma\text{-Ni}$ and $\gamma'\text{-Ni}_3\text{Al}$ phases each occupying a half of the supercell. In the Re-doped structure, one Ni atom on the $(002) \gamma/\gamma'$ interfacial layer (layer number 0) was substituted by a Re atom.

iments using aberration-corrected high-angle annular dark-field scanning transmission electron microscopy (HAADF-STEM) [36] and three-dimension atom-probe tomography (3D-APT) [37], we set up an atomic calculation model for the computation of energetic parameters and electronic structure from DFT approach. A diagram of the geometric model is depicted in Fig. 1.

The HAADF-STEM images are shown in Fig. 2a for the Re-doped $\text{Ni}_3\text{Al}/\text{Ni}$ (γ'/γ) superalloy. In general, the concentration of Re is less than 2 at%. The abovementioned experiments indicate that the Re atoms can be distributed in the γ' phase (Ni_3Al) and the γ phase (Ni matrix), and at the γ'/γ connecting region. On the fact, we chose to substitute Ni with Re in the connecting region between the γ' and γ phases. From the HAADF-STEM experimental information, we used the singular value decomposition technique to treat the data of the diffraction point in distinguishing the type of chemical element. The experiment results are shown in Fig. 2b with Re atoms marked in red and Re pairs in yellow and the experiment indicates that the coherent interface for γ'/γ can be easy to found. In addition, our 3D-APT experiments (Fig. 3) indicate that the Re atoms are distributed in the $\gamma'(\text{Ni}_3\text{Al})$ phase, $\gamma(\text{Ni})$ phase, and γ/γ' conjunction region. In the model, we paid particular attention to the influence of dopant Re on the diffusion behavior of Ni and Al atoms. We found that vacancy diffusion dominates the behavior of Ni and Al atoms in the matrix γ phase and in the intermetallic compound $\gamma'\text{-Ni}_3\text{Al}$ phase, respectively [19].

3 Theoretical calculation methods with relevant mainly expressions

For the study of the diffusion behavior in single crystals of Ni-based superalloys and Re doping in the Ni matrix (γ phase) of the system studied, we used a correlation scheme combining the transition state theory (TST) with DFT approach and the KMC method.

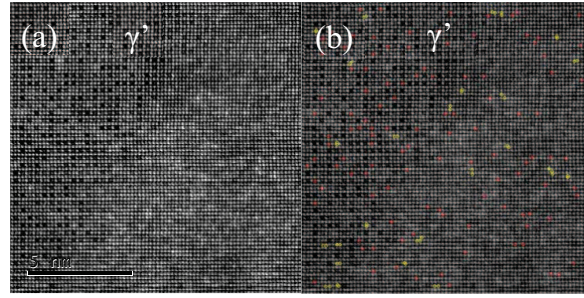


Figure 2: STEM-HAADF images of the Ni-Al-Re alloy. (a) Unmarked, (b) Marked.

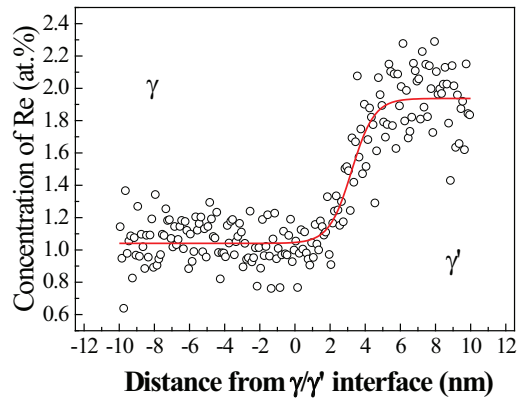


Figure 3: Concentration profile of Re.

The basic idea and computational equations used are given below; for more details readers are referred to [2, 19, 22, 23, 38–43].

3.1 Basic theoretical consideration and relevant equations for first-principles calculations

The key energy parameters related to diffusion behavior can be obtained from Vienna ab initio simulation package (VASP) [44, 45] using the projector augmented wave (PAW) method [46, 47].

3.1.1 Energy of vacancy formation

The calculation equation directly related with the vacancy diffusion mechanism describes the energy in vacancy formation. In solids, each atom moves through the crystal lattice site, needing to perform a series of exchanges with neighboring vacancy sites from time to time. In the thermal equilibrium state, the site fraction of vacancies in a mono-atomic

crystal can be given by the ground-state approximation in DFT, that is [2, 19, 48],

$$C_V^{eq} = \exp\left(-\frac{E_V^f}{k_B T}\right), \quad (3.1)$$

where E_V^f is the energy of vacancy formation. Hence, the fraction of vacancies increases with increasing temperature via the Boltzmann factor. The energy in vacancy formation for Ni atoms in a matrix Ni (γ phase) can be expressed in sample form [10, 11]

$$(E_V^f)_{Ni} = E_{system}(with \text{ a vacancy}) - E_{system}(pure), \quad (3.2)$$

whereas for a dilute substitutional alloy with a vacancy and a vacancy near a solute Al atom, we have the expression

$$(E_V^f)_{Al} = E_{system}(with \text{ a vacancy}) - E_{system}(dilute \text{ substitutional Ni - Al binary alloy}). \quad (3.3)$$

In the dilute substitutional alloy, the site fraction of vacancies can be given by the Lomer equation [19, 49]

$$C_{vacancy}^{eq}(C_{solute}) = \exp\left(-\frac{E_V^f(matrix)}{k_B T}\right) \left[1 - ZC_{solute} + ZC_{solute} \exp\left(\frac{E^{solute}}{k_B T}\right)\right], \quad (3.4)$$

where C_{solute} is the concentration of the solute atoms, Z the coordination number, and E^{solute} the interaction energy between solute and vacancy defined as

$$E^{solute} = E_V^f(matrix) - E_V^f(solute). \quad (3.5)$$

3.1.2 Energy of migration of an atom

The second key energy parameter for the diffusion problem in solids is the energy in the migration of atoms. Jump processes need a driving energy that is sufficient to overcome lattice barriers and prompt diffusion; at which point the diffusing atom accomplishes a successful jumping motion. Thermally activated motion of atoms in a crystal appears as a series of discrete jumps from one lattice site to another neighboring site [19, 23, 41]. Jumps can be viewed as an atom jumping from a potential well to the saddle point; the energy required is called as the saddle energy of migration of atom and can be written

$$E^m = V_{barrier} - V_{well} = E_{saddle}. \quad (3.6)$$

The saddle energy can be obtained from TST with the climbing image nudged elastic band method [40].

3.1.3 Diffusion behavior in the L1₂ intermetallic compound Ni₃Al

In Ni₃Al, each Ni atom has eight nearest-neighbor (N-N) Ni atoms and four N-N Al atoms; their neighboring atoms form an interconnected N-N sublattice of bonds but the neighboring sites for each Al atom do not form an interconnected N-N sublattice. From energetics alone, this implies that the sublattice of Ni atoms would have preference. The Ni₃Al is a strengthening phase in Ni-based superalloys, in which the diffusion of atoms is very important in determining mechanical properties, such as creep and fracture. Considering Ni₃Al belongs to the class of antistructural defect-type intermetallics [19,50] and considering the energy of vacancy formation for Ni and Al, we can suppose vacancies form preferably in the Ni sublattice and hence the atoms, Ni or Al, will diffuse preferably via sublattice vacancies [19–21].

Based on the above discussion, the equations governing the site fraction of vacancies in Ni sublattice of Ni₃Al intermetallic take the form given in Eqs. (3.1) and (3.4) for Ni and Al atoms, respectively. For the diffusion of Ni atom, in particular, the energy of vacancy formation is calculated from Eq. (3.2) whereas for the diffusion of Al atoms, the energy of vacancy formation is obtained from Eq. (3.3). The energy of migration for the intermetallic Ni₃Al system is given by Eq. (3.6).

3.1.4 Transition rate in diffusion process of solids [19]

Based on the Vineyard [23] and TST, the transition rate can be expressed as [23,41]

$$\omega^{JP} = v^0 \exp\left(-\frac{E^m}{k_B T}\right), \quad (3.7)$$

where ω^{JP} is the number of jumps per unit time to a neighboring site and v^0 , called the attempt frequency, has typical values in the range 10^{12} – 10^{13} Hz for metals, which is of the order of the Debye frequency [19,30,51].

Based on the energies for vacancy formation and migration, we derive an expression for the transition rate for an atom moving to a neighboring site under sublattice vacancy diffusion in the form

$$\omega_{exchange}^{JR} = \omega^{JR} C_V^{eq} = v^0 \exp\left(-\frac{E^m}{k_B T}\right) C_V^{eq} = v^0 \exp\left(-\frac{E^m + E_V^f}{k_B T}\right), \quad (3.8)$$

where $E^m + E_V^f = E^{activation}$.

3.2 Kinetic Monte Carlo method with DFT in diffusion analysis

The interesting of KMC is that it can give the dynamical evolution behavior and present the physical process in diffusion of solid state. The most key point of KMC lies in that it can overcome the time-scale limit of MD simulation and to explore the long-time correlation between physical parameters and then to treat the trajectory of state-to-state transitions of the entire system.

3.2.1 Characteristic parameter governing diffusion – Transition Rate

In this work, the correlation scheme combining the DFT with the KMC method is established. For the diffusion process calculated from DFT, the important parameters are, for example, the energy of vacancy formation, the site fraction of vacancies in the crystal, the energy of migration of an atom (the saddle energy), and the activation energy in the jump process of atoms. In combining the DFT with KMC method, the main task is finding a characteristic parameter. Here, we show that an equivalent expression for the transition rate can be formulated from the theory of diffusion in solids [19, 23, 39] and the KMC method [22, 40], respectively. Specifically, the transition rate from the theory of solid diffusion within DFT is given by

$$\omega_{exchange}^{JR} = \omega^{JR} C_{1V}^{eq} = v^0 \exp\left(-\frac{E^m + E_V^f}{k_B T}\right). \quad (3.9)$$

In the HTST [22, 23, 52] which introduces the partition function on i state and saddle state respectively, and according to the Boltzmann equation with the evolution of the ensemble average for a system with N moving atoms, a formulation for the equivalent transition rate from i state to j state can be expressed as

$$k_{ij} = \left[\frac{\prod_{i=1}^{3N} v_{ij}^0}{\prod_{i=1}^{3N-1} v_{ij}^{sad}} \right] \exp\left(-\frac{E_{ij}}{k_B T}\right), \quad (3.10)$$

where $E_{ij} = E^m + E_V^f$. Because of the length of calculation, the pre-factor in Eq. (3.10) can be taken as a constant, then the equation of the transition rate as

$$k_{ij} = v^0 \exp\left(-\frac{E_{ij}}{k_B T}\right) = v^0 \exp\left(-\frac{E^m + E_V^f}{k_B T}\right). \quad (3.10')$$

In general, the v^0 takes the value 10^{12} Hz (that approaches the Debye frequency) [19, 30, 51]. Assuming vacancy diffusion in metals, Eq. (3.10) is then equivalent to Eq. (3.9).

3.2.2 Transition rate with time step in the KMC method

Kinetic simulations are the important scientific computational methods, which involve in temperature and time. The KMC method possesses especial significance in the study of diffusion in materials, its advantages in diffusion simulations overstep the molecular dynamics method. Focusing on the configuration transition process of a system, the simulation time covers intervals from the atom vibration scale to the configuration hopping scale; the timescale for configuration transitions are directly correlated with transition rate k_{ij} [22, 42]. In the KMC method, if k_{ij} are known, the random process can be constructed. Indeed, the KMC method principally involves constructing a random processes

to study the evolution of a system and to understand diffusion behaviors within metals and alloys.

In detail, we need to construct a random distribution of exponential-type events. Based on analytical work [22,53,54], the transition probability per unit time of the system is

$$P(t) = k_{tot} \exp(-k_{tot}t). \quad (3.11)$$

Here

$$k_{tot} = \sum_j k_{ij} \quad (3.12)$$

which represents the transition rate for all possible jump paths. As for the transition probability per unit time in the system from state i to state j , based on Eq. (3.11) and Eq. (3.12), we can define as

$$P_{ij}(t) = k_{ij} \exp(-k_{ij}t). \quad (3.13)$$

To obtain the time step, a set of random numbers that appear in the exponentials is required. For this purpose, we need a mapping of the set of random numbers taken from a uniform distribution on the interval $[0,1]$ into the form

$$r = 1 - F_{stay}(k_{tot}\delta t), \quad (3.14)$$

where $1 - F_{stay}(k_{tot}\delta t)$ is the probability that the jump can occur in the system. Within the KMC method, $F_{stay}(k_{tot}\delta t)$ which is the probability that the jump cannot occur in the system can be expressed as [22]

$$F_{stay}(k_{tot}\delta t) = \exp(-k_{tot}\delta t). \quad (3.15)$$

Taking the logarithm of Eq. (3.14), we have

$$\delta t = -\frac{1}{k_{tot}} \ln(1-r) = -\frac{1}{k_{tot}} \ln(r). \quad (3.16)$$

The correlation between the transition probability and the time step is established and the characteristic time can be obtained.

3.2.3 Calculations of the coefficient of diffusion

Diffusion occurring in solids through the motion of atoms induced by thermal fluctuations has a statistical nature. According the Einstein-Smoluchowski (ES) relation [19], the mean square displacement of atoms is directly related with the coefficient of diffusion. The sequential jumps of the atoms between neighboring lattice sites results in macroscopic diffusion, the sublattice vacancy diffusion being the dominant mechanism in metals. Based on the ES relation with Fick's second law, the coefficient of diffusion can be written as

$$D_X = \frac{\langle X^2 \rangle}{\Delta t}, \quad (3.17)$$

where $\langle X^2 \rangle$ is mean square displacement specified along the X direction. For an isotropic medium and without a driving force, the mean square displacement can be expressed as

$$\langle X^2 \rangle = \langle Y^2 \rangle = \langle Z^2 \rangle = \frac{1}{3} \langle R^2 \rangle, \quad (3.18)$$

where $R^2 = X^2 + Y^2 + Z^2$ is the displacement length and the coefficient of diffusion can be calculated by

$$D_X = \frac{\langle R^2 \rangle / 3}{2t} = \frac{\langle R^2 \rangle}{6t}, \quad (3.19)$$

where $\langle R^2 \rangle$ is total mean square displacement and t the simulation time in the KMC simulation.

4 Calculational results and discussion

4.1 Density functional theory calculations

4.1.1 Theoretical method

Recall that E_V^f and E^m are obtained using VASP and the PAW method, in addition to the generalized gradient approximation for the exchange-correlation potential [55]. The computational model is a unit cell of 160 atoms constructed along the $\langle 001 \rangle$ direction (Fig. 1). The supercell is equally divided by a (002) interface, phases γ -Ni and γ' -Ni₃Al each occupy one half of the supercell. In assuming complete coherence, the lattice parameters of the supercell are taken to be the same for both phases [56]. Taking into account that the enhancement in creep performance occurs mainly related with the strengthening of the alloying element in the γ - γ' connecting region, a model with one Re atom on the γ - γ' connecting was constructed to investigate the effect of Re on the diffusion of Ni and Al atoms across the connecting region. In this Re-doped model, one Ni atom on the (002) interfacial layer is substituted by a Re atom (Fig. 1).

In calculations, a plane-wave cutoff energy of 350.5 eV was used that yielded convergent results. The K points were sampled according to the Monkhorst-Pack scheme [57] with a $1 \times 6 \times 6$ k -mesh. The structures were relaxed by minimizing the total energy with a convergence accuracy of 10^{-4} eV. The climbing image nudged elastic band method [40] was used to obtain the energy of migration of the Re atom. The structure was relaxed until the maximum residual forces were less than 0.02 eV/Å.

4.1.2 Energy of vacancy formation

Note that the energy of vacancy formation can be viewed as a guide in choosing the atom diffusion matrix for a solid. From DFT calculations, the energy of vacancy formation for Al is larger than that for Ni in the intermetallic compound Ni₃Al (γ' phase). We can then suppose that atom diffusion for either atom in the γ' phase proceeds via the Ni-sublattice.

4.1.3 Energy of migration of atom

From a previous study [19], we understand E^m as determining the capability of an atom to overcome barriers during diffusion, and that it is closely related to the saddle point of the calculated crystal lattice which is correlated with the electronic configuration of the atom. Table 1 shows that the climbing barrier capability of a Ni atom in the γ and γ' phases both of which are stronger than that of the Al atom.

Table 1: Comparison of calculated E_V^f and E^m (in eV) of Ni and Al diffusion in matrices Ni and Ni₃Al, as well as Re in the γ/γ' connecting region, with results from other theoretical analysis and experiments.

		E_V^f			E^m			Q		
		present			present			present		
		work	other	experiment	work	other	experiment	work	other	experiment
Matrix Ni or Ni ₃ Al	Ni in Ni	1.51	1.71 ^a	1.70 ^d	0.93	1.15 ^a	1.04 ^f	2.44	2.86 ^a	2.10 ^f
			1.39 ^b	1.55±0.05 ^e		0.97 ^g				2.87 ^h
			1.51 ^c	1.60 ^f						
	Al in Ni	1.50	1.56 ⁱ		0.72	0.66 ⁱ		2.22	2.22 ⁱ	3.55±0.13 ^j
	Ni in Ni ₃ Al	1.59 ^k	1.58 ^l	1.81±0.08 ^o	0.97	0.95 ^l	1.20±0.4 ^p	2.70	2.53 ^{kl}	2.80±0.4 ^p
			1.70 ^m	1.60 ^p						2.51 ^q
			1.61 ⁿ							
		Al in Ni ₃ Al	1.80 ^k		0.80			2.58		
Re in γ/γ' connecting region	Ni in Ni	1.51			1.05			2.56		
	Al in Ni	1.44			0.46			1.90		
	Ni in Ni ₃ Al	1.70			1.25			2.95		
	Al in Ni ₃ Al	1.63			0.27			1.89		

^aRef. [8], ^bRef. [11], ^cRef. [58], ^dRef. [59], ^eRef. [60], ^fRef. [61], ^gRef. [62], ^hRef. [63],

ⁱRef. [64], ^jRef. [65], ^kRef. [10], ^lRef. [66], ^mRef. [67], ⁿRef. [10], ^oRef. [68], ^pRef. [69], ^qRef. [70].

4.1.4 Effect of heavy element Re

Considering the electronic configuration and atomic mass, we can easily understand that the Re atom will restrict the ability of atom diffusion and influence the diffusion coefficients appearing in our calculated results. In particular, considering that most of the Ni atoms reside in the superalloy, then the element Re is strongly suppressed the capability of diffusion over the entire system.

Concerning the effect of Re on the diffusion of Al, we see from the calculated results listed in Table 2. In order to explain the physical ground, bond order corresponding the interaction energy is calculated by DMol3 [71,72]. The calculated results indicate that the value of the bond order between the Re atom and Ni atom is 0.393, and between the Re atom and Al atom is 0.276. Obviously the influence of diffusion capacity of Re on Ni atoms is a restricting effect, but for Al atoms the effect can be negligible.

Table 2: Atomic diffusivity (units in m^2/s) for Ni and Al in the γ and γ' phase at temperatures 300 K, 1000 K, and 1400 K obtained from KMC simulations. Obtained from experiments, the impurity fraction C_{Al} is set to 10%.

	State of diffusion system	Ni in γ	Ni in γ'	Al in γ	Al in γ'
$T=300\text{K}$	Matrix Ni and Ni_3Al	1.3×10^{-48}	8.2×10^{-51}	6.7×10^{-45}	5.8×10^{-48}
	Re in γ/γ' connecting region	1.5×10^{-50}	1.9×10^{-57}	2.3×10^{-39}	1.1×10^{-39}
$T=1000\text{K}$	Matrix Ni and Ni_3Al	6.3×10^{-20}	1.0×10^{-20}	8.2×10^{-19}	7.5×10^{-20}
	Re in γ/γ' connecting region	1.6×10^{-20}	1.1×10^{-22}	4.0×10^{-17}	2.1×10^{-17}
$T=1400\text{K}$	Matrix Ni and Ni_3Al	2.0×10^{-16}	5.0×10^{-17}	1.3×10^{-15}	2.1×10^{-16}
	Re in γ/γ' connecting region	7.9×10^{-17}	1.9×10^{-18}	2.1×10^{-14}	1.2×10^{-14}

4.1.5 Effect of atomic mass and temperature

Also from the calculated results, the atom diffusion process in solids and superalloy show a sensitive dependence on mass and temperature, the latter being a key factor in atomic diffusion within solids. Our calculations show that the values for the coefficient of diffusion rise strongly with increasing temperature.

4.2 Kinetic Monte Carlo calculations

4.2.1 Theoretical KMC method

Performing KMC simulations of atomic diffusion requires two random numbers which need to be generated at each step; one for the transition path, and the other for the time step δt from $\delta t = -\ln(r)/k_{tot}$, where k_{tot} is the sum of rates for all possible transitions with r a random number. The transition rates k_{ij} and diffusion process are calculated from Eqs. (3.9) to (3.19).

4.2.2 Calculation results and discussion

In examining the atomic diffusivity from the KMC simulations, three temperature conditions are considered: room temperature of $T=300\text{ K}$, a medium temperature of $T=1000\text{ K}$, and a typical working temperature in experiments of $T=1400\text{ K}$. The atomic diffusivity is calculated using Eq. (3.18) with averages taken over 10^5 KMC trajectories. In each trajectory, 10^5 transitions are considered, which corresponds to a diffusion length of $0.1\text{ }\mu\text{m}$ and a diffusion time of around 10 second (i.e., $\sim 10^{-4}$ second for each time step) for $T=1400\text{ K}$. The calculated atomic diffusivities (Table 2) are listed for the γ phase (matrix Ni) and γ' phase (intermetallic compounds), as well as those for the γ - γ' connecting region doped with Re. We investigated the effect of Re on atom diffusivity, with the energies of migration and vacancy formation taken from the values at layers 1 and -1 in the γ - γ' connecting region (Fig. 1).

From Table 2, the diffusivity is higher for Al than for Ni; both atoms show a higher diffusivity in the γ phase than in the γ' phase. These results stem mainly from their dif-

Table 3: Dependence of Al diffusivity (unit in m^2/s) in γ phase on the Al impurity fraction.

Al concentration (at.%)		0.1%	1%	10%
$T = 300\text{K}$	Matrix Ni	4.3×10^{-45}	4.5×10^{-45}	6.7×10^{-45}
	Re in γ/γ' connecting region	1.4×10^{-40}	3.3×10^{-40}	2.3×10^{-39}
$T = 1000\text{K}$	Matrix Ni	7.2×10^{-19}	7.3×10^{-19}	8.2×10^{-19}
	Re in γ/γ' connecting region	1.5×10^{-17}	1.8×10^{-17}	4.0×10^{-17}
$T = 1400\text{K}$	Matrix Ni	1.2×10^{-15}	1.2×10^{-15}	1.3×10^{-15}
	Re in γ/γ' connecting region	1.0×10^{-14}	1.1×10^{-14}	2.1×10^{-14}

ferent diffusion barriers, as discussed above. Furthermore, we find that the diffusivity around the γ - γ' connecting region is different from that in the γ and γ' phases, and the doping of Re reduces the diffusivity of Ni in both γ and γ' phases. The atomic diffusivity is also strongly dependent on temperature. From $T = 300\text{ K}$ to $T = 1400\text{ K}$, the diffusivity changes from $\sim 10^{-48}\text{ m}^2/\text{s}$ to $\sim 10^{-17}\text{ m}^2/\text{s}$ for Ni in the γ phase.

We also examined the diffusivity dependence on the Al-atom fraction (Table 3). Here, three atom fractions 0.1%, 1%, and 10% are considered. From Eq. (3.4), the transition rate depends on the atom fraction C_{Al} , which is evident in the results of Table 3.

5 Summary

We close with the following remarks from our study of DFT calculations and KMC simulations of Ni-based superalloys:

1. A correlation scheme combining the TST with DFT and the KMC method is established. We used this theoretical model to study alloying compositions in superalloys and to select heat treatment technologies, as well as to explore the stability of alloy phases in regard to creep behavior.
2. An equivalent expression for the transition rate, a key parameter in governing diffusion in solids, is formulated from the TST with DFT and KMC method in the paper. The transition rate bridges DFT calculations and KMC simulations of alloy diffusion in superalloys.
3. Based on our DFT calculations, the energy of vacancy formation is useful as a guide in choosing the matrix appropriate for atom diffusion in intermetallic compound Ni_3Al of a superalloy. We can regard Ni and Al diffusion in Ni_3Al as sublattice vacancy diffusion through the sublattice of the Ni.
4. Re-doping of the γ - γ' connecting region at substitutional Ni sites results in suppression of Ni diffusion, which is demonstrated by our calculation results. Considering that Ni is the main constitute of the superalloy, we suggest that a Re-doped superalloy strongly lowers atom diffusivity throughout the superalloy thereby increasing the structural stability of the alloy phases with creep.

5. Temperature is another key factor in superalloy diffusion. Our calculation results indicate that diffusivity rises strongly with increasing temperature. The diffusion at 300 K reflects the stability of γ' and γ phases of the superalloy. Like the effect of temperature on diffusion, the atomic mass has only an inverse effect. That is, Re and Ni both sensitively influence the ability of atom diffusion. Nevertheless, Al possesses a higher diffusivity than Re and Ni.
6. Finally, based on our calculation results, we find that the time step (δt) for the superalloy system at 1400 K is 10^{-4} s, which suggests that the multi-time scaling parameter δt is a very important physical parameter that can be included in the correlated scheme for DFT calculations and KMC simulations.

Acknowledgments

This work was supported by the National Basic Research Program of China (Grant No. 2011CB606402). Many thanks to Doctor Zheng Zheng Chen (California State University) for enthusiastically supporting this work.

References

- [1] R. C. Reed. The Superalloys: Fundamentals and Applications. New York: Cambridge University Press; 2006.
- [2] P. Shewmon. Diffusion in Solids. 2nd TMS, Warrendale, PA; 1989, p.223.
- [3] Y. Wang, Z. K. Liu and L. Q. Chen. Thermodynamic properties of Al, Ni, NiAl, and Ni₃Al from first-principles calculations. *Acta Mater.* 2004; 52:2665-2671.
- [4] T. Zhu, C. Y. Wang, Y. Gan, Effect of Re in γ phase, γ' phase and γ/γ' interface of Ni-based single-crystal superalloys, *Acta Mater.* 2010; 58:2045-2055.
- [5] A. Ziegler, J. C. Idrobo, M. K. Cinibulk, C. Kisielowski, N. D. Browning, R. O. Ritchie. Interface structure and atomic bonding characteristics in silicon nitride ceramics. *Science* 2004; 306:1768-1770.
- [6] R. Srinivasan, R. Banerjee, J. Y. Hwang, G. B. Viswanathan, J. Tiley, D. M. Dimiduk, H. L. Fraser. Atomic scale structure and chemical composition across order-disorder interfaces. *Phys. Rev. Lett.* 2009; 102:086101.
- [7] H. Y. Yasuda, H. Nakajima, M. Koiwa. Diffusion in L12-type intermetallic compounds. *Defect Diffus. Forum.* 1993; 95:823-830.
- [8] M. Krčmar, C. L. Fu, A. Janotti, R. C. Reed. Diffusion rates of 3D transition metal solutes in nickel by first-principles calculations. *Acta Mater.* 2005; 53:2369-2376.
- [9] M. Mantina, Y. Wang, L. Q. Chen, Z. K. Liu, C. Wolverton. First principles impurity diffusion coefficients, *Acta Mater.* 2009; 57:4102-4108.
- [10] X. Zhang, C. Y. Wang. First-principles study of vacancy formation and migration in clean and Re-doped γ' -Ni₃Al. *Acta Mater.* 2009; 57:224-231.
- [11] X. X. Yu, C. Y. Wang. The effect of alloying elements on the dislocation climbing velocity in Ni: A first-principles study. *Acta Mater.* 2009; 57:5914-5920.
- [12] T. Zhu, C.-Y. Wang. Misfit dislocation networks in the γ/γ' phase interface of a Ni-Based single-crystal superalloys: Molecular dynamics simulations. *Phys. Rev. B* 2005; 72:014111.

- [13] J. P. Du, C. Y. Wang, T. Yu. Construction and application of multi-elements EAM potential (Ni-Al-Re) in γ/γ' Ni-based single crystal superalloys. *Modelling Simul. Mater. Sci. Eng.* 2013; 21:015007.
- [14] Z.-G. Liu, C.-Y. Wang, T. Yu. Molecular dynamics simulations of influence of Re on lattice trapping and fracture stress of cracks in Ni. *Comput. Mater. Sci.* 2014; 83:196-205.
- [15] S. L. Liu, C. Y. Wang, T. Yu. Influence of the alloying elements Re, Co and W on the propagation of the Ni/Ni₃Al interface crack. *RSC Advances* 2015; 5:52473-52480.
- [16] C. Wang, C.-Y. Wang. Ni/Ni₃Al interface: A density functional theory study. *Applied Surface Science* 2009; 255:3669-3675.
- [17] Y.-J. Wang, C.-Y. Wang. A comparison of the ideal strength between L₁₂Co₃(Al,W) and Ni₃Al under tension and shear from first-principles calculations. *Applied Physics Letters* 2009; 94:261090.
- [18] X. Wu, C. Y. Wang. Density functional theory study of the thermodynamic and elastic properties of Ni-based superalloys. *J. Phys.: Condensed Matter* 2015; 27:295401.
- [19] H. Mehrer. *Diffusion in solids: Fundamentals, methods, materials, diffusion-controlled processes.* Springer Science & Business Media, 2007, p.56-65, 70-72, 80-82, 98-99, 327-331, 355-357.
- [20] M. Koiwa, H. Numakura, S. Ishioka. Diffusion in L₁₂ type intermetallic compounds. *Defect and Diffusion Forum.* 1997; 143:209-222.
- [21] M. Koiwa, S. Ishioka. Random walks and correlation factor in diffusion in a three-dimensional lattice with coordination number 8. *Philos. Mag. A* 1983; 48:1-9.
- [22] A. F. Voter. *Radiation Effects in Solids.* Edited by K. E. Sickafus, E. A. Kotomin, B. P. Uberuaga. Dordrecht: Springer, NATO Publishing Unit, 2006; p. 1-24.
- [23] G. H. Vineyard. Frequency factors and isotope effects in solid state rate processes. *J. Phys. Chem. Solids*, 1957; 3:121-127.
- [24] K. A. Fichtorn, W. H. Weinberg. Theoretical foundations of dynamical Monte Carlo simulations. *J. Chem. Phys.*, 1991; 95:1090.
- [25] W. M. Young, E. W. Elcock. Monte Carlo studies of vacancy migration in binary ordered alloys: I. *Proc. Phys. Soc.* 1966; 89:735.
- [26] W. Kinzel, W. Selke, K. Binder. Phase transitions on centered rectangular lattice gases: A model for the adsorption of H on Fe(110). *Surf. Sci.* 1982; 121:13.
- [27] P. S. Sahni, G. S. Grest, S. A. Safran. Temperature dependence of domain kinetics in two dimensions. *Phys. Rev. Lett.*, 1983; 50:60.
- [28] V. S. Stepanyuk, N. N. Negulyaev, L. Niebergall, R. C. Longo, P. Bruno. Adatom self-organization induced by quantum confinement of surface electrons. *Phys. Rev. Lett.*, 2006; 97:186403.
- [29] M. Ziegler, J. Kröger, R. Berndt, A. Filinov, M. Bonitz. Scanning tunneling microscopy and kinetic Monte Carlo investigation of cesium superlattices on Ag(111). *Phys. Rev. B* 2008; 78:245427.
- [30] Z. Chen, N. Kioussis, K.-N. Tu, N. Ghoniem, J.-M. Yang. Inhibiting adatom diffusion through surface alloying. *Phys. Rev. Lett.* 2010; 105:015703.
- [31] P. K. Watkins, A. B. Walker, and G. L. B. Verschoor. Dynamical Monte Carlo modelling of organic solar cells: The dependence of internal quantum efficiency on morphology. *Nano Lett.* 2005; 5:1814.
- [32] X. Zhang, Z. Li, G. Lu. First-principles simulations of exciton diffusion in organic semiconductors. *Phys. Rev. B* 2011; 84:235208.
- [33] A. F. Voter. Classically exact overlayer dynamics: Diffusion of rhodium clusters on Rh(100).

- Phys. Rev. B 1986; 34:6819.
- [34] G. DeLorenzi, C. P. Flynn, G. Jacucci. Effect of anharmonicity on diffusion jump rates. Phys. Rev. B 1984; 30:5430.
- [35] M. R. Sørensen, A. F. Voter. Temperature-accelerated dynamics for simulation of infrequent events. J. Chem. Phys. 2000; 112:9599.
- [36] R. Srinivasan, R. Banerjee, J. Y. Hwang, G. B. Viswanathan, J. Tiley, D. M. Dimiduk, H. L. Fraser. Atomic scale structure and chemical composition across order-disorder interfaces. Phys. Rev. Lett. 2009; 102:086101.
- [37] R. C. Reed, A. C. Yeh, S. Tin, S. S. Babu, M. K. Miller. Identification of the partitioning characteristics of ruthenium in single crystal superalloys using atom probe tomography. Scripta Materialia 2004; 51:327-331.
- [38] X. X. Yu, C. Y. Wang, X. N. Zhang, P. Yan, Z. Zhang. Synergistic effect of rhenium and ruthenium in nickel-based single-crystal superalloys, J. Alloys Compd. 2014; 582:299-304.
- [39] A. C. Yeh, S. Tin. Effects of Ru and Re additions on the high temperature flow stresses of Ni-base single crystal superalloys, Scripta Materialia 2005; 52:519-524.
- [40] G. Henkelman, B. P. Uberuaga, H. Jónsson. A climbing image nudged elastic band method for finding saddle points and minimum energy paths. J. Chem. Phys. 2000; 113:9901-9904.
- [41] C. A. Wert. Diffusion Coefficient of C in α -Iron. Phys. Rev. 1950; 79:601.
- [42] H. Eyring. The activated complex in chemical reactions. J. Chem. Phys. 1935; 3:107-115.
- [43] Z. Li, X. Zhang, F. Cristiano, W. G. Lu. Understanding molecular structure dependence of exciton diffusion in conjugated small molecules. Appl. Phys. Lett. 2014; 104:143303.
- [44] G. Kresse, J. Hafner. Ab initio molecular dynamics for liquid metals. Phys. Rev. B 1993; 47:558.
- [45] G. Kresse, J. Furthmüller. Efficient iterative schemes for ab initio total-energy calculations using a plane-wave basis set. Phys. Rev. B 1996; 54:11169.
- [46] P. E. Blöchl. Projector augmented-wave method. Phys. Rev. B 1994; 50:17953.
- [47] G. Kresse, D. Joubert. From ultrasoft pseudopotentials to the projector augmented-wave method. Phys. Rev. B 1999; 59:1758.
- [48] W. Kohn, L. J. Sham. Self-consistent equations including exchange and correlation effects. Phys. Rev. 1965; 140:A1133-A1138.
- [49] W. M. Lomer. Vacancies and other point defects in metals and alloys. Institute of Metals, London, 1958; 79.
- [50] C. Herzig, S. Divinski. Diffusion in Intermetallic Compounds in: Diffusion Processes in Advanced Technological Materials. William Andrew, Inc., 2005.
- [51] P. Zhang, Y. Xu, F. Zheng, S. Q. Wu, Y. Yang, Z. Z. Zhu. Ion diffusion mechanism in $\text{Pn Na}_x\text{Li}_{2-x}\text{MnSiO}_4$. Cryst. Eng. Comm. 2015; 17:2123-2128.
- [52] P. Hanggi, P. Talkner, M. Borkovec. Reaction-rate theory: Fifty years after Kramers. Rev. Mod. Phys. 1990; 62:251.
- [53] D. T. Gillespie. Multiscale stochastic simulation algorithm with stochastic partial equilibrium assumption for chemically reacting systems. J. Comp. Phys. 1976; 22: 403.
- [54] K. A. Fichthorn, W. H. Weinberg. Theoretical foundations of dynamical Monte Carlo simulations. J. Chem. Phys. 1991; 95: 1090.
- [55] J. P. Perdew, K. Burke, M. Ernzerhof. Generalized gradient approximation made simple. Phys. Rev. Lett. 1996; 77:3865.
- [56] H. Harada, A. Ishida, Y. Murakami, H. K. D. H. Bhadeshia, M. Yamazaki. Atom-probe microanalysis of a nickel-base single crystal superalloy. Appl. Surf. Sci. 1993; 67:299-304.
- [57] H. J. Monkhorst, J. D. Pack. Special points for Brillouin-zone integrations. Phys. Rev. B 1976;

- 13:5188.
- [58] B. J. Lee, J. H. Shim, M. I. Baskes. Semiempirical atomic potentials for the fcc metals Cu, Ag, Au, Ni, Pd, Pt, Al, and Pb based on first and second nearest-neighbor modified embedded atom method. *Phys. Rev. B* 2003; 68:144112.
 - [59] L. C. Smedskjaer, M. J. Fluss, D. G. Legnini, M. K. Chason, R. W. Siegel. *Positron Annihilation*. Amsterdam: North-Holland; 1982.
 - [60] K. Maier, M. Peo, B. Saile, H. E. Schaefer, A. Seeger. High-temperature positron annihilation and vacancy formation in refractory metals. *Philos. Mag. A* 1979; 40:701-728.
 - [61] W. Wycisk, M. F. Kniepmeier. Quenching experiments in high purity Ni. *J. Nucl. Mater.* 1978; 69:616-619.
 - [62] M. G. Ortega, S. B. Ramos de Debiaggi, A. M. Monti. Self-Diffusion in FCC Metals: Static and dynamic simulations in aluminium and nickel. *Phys. Status Solidi (b)* 2002; 234:506.
 - [63] C. J. Smithells. *Metals Reference Book*, seventh ed. Oxford: Butterworth-Heinemann; 1992.
 - [64] Q. Wu, S. S. Li, Y. Ma, S. K. Gong. First principles calculations of alloying element diffusion coefficients in Ni using the five-frequency model. *Chin. Phys. B* 2012; 21:109102.
 - [65] W. Gust, M. B. Hintz, A. Loddwg, H. Odelius, B. Predel. Impurity diffusion of Al in Ni single crystals studied by secondary ion mass spectrometry (SIMS). *Phys. Status Solidi (a)* 1981; 64:187-194.
 - [66] X. F. Gong, G. X. Yang, Y. H. Fu, Y. Q. Xie, J. Zhuang, X. J. Ning. First-principles study of Ni/Ni₃Al interface strengthening by alloying elements. *Comput. Mater. Sci.* 2009; 47:320-325.
 - [67] F. Cardellini, F. Cleri, G. Mazzone, A. Montone, V. Rosato. Experimental and theoretical investigation of the order-disorder transformation in Ni₃Al. *J. Mater. Res.* 1993; 8:2504-2509.
 - [68] K. Badura-Gergen, H. E. Schaefer. Thermal formation of atomic vacancies in Ni₃Al. *Phys. Rev. B* 1997; 56:3032.
 - [69] T. M. Wang, M. Shimotomai, M. Doyama. Study of vacancies in the intermetallic compound Ni₃Al by positron annihilation. *J. Phys. F: Metal Phys.* 1984; 14:37.
 - [70] G. X. Chen, D. D. Wang, J. M. Zhang, H. P. Huo, K. W. Xu. Self-diffusion of Ni in the intermetallic compound Ni₃Al. *Physica B* 2008; 403:3538-3542.
 - [71] Delley B. An all-electron numerical method for solving the local density functional for polyatomic molecules. *J. Chem. Phys.* 1990; 92:508-517.
 - [72] Delley B. Analytic energy derivative in the numerical local-density-functional approach. *J. Chem. Phys.* 1991; 94:7245-7250.